THE UNIVERSITY of EDINBURGH

Edinburgh Research Explorer

The supramolecular and coordination chemistry of cobalt(II) extraction by phosphinic acids

OPEN ACCESS

The supramolecular and coordination chemistry of cobalt(II) extraction by phosphinic acids

Innis Carson[a], Peter A. Tasker[a], Jason B. Love[a], Michael Moser[b], Adam J. Fischmann[b], Boban Jakovljevic[c], Matthew D. Soderstrom[d], Carole A. Morrison[a, *]

[a]School of Chemistry and EaStCHEM Research School, University of Edinburgh, David Brewster Road, Edinburgh, EH9 3FJ

[b]Solvay Metal Extraction Products, 1937 W Main St, Stamford, CT 06902, USA

[c]Solvay Metal Extraction Products, 9061 Garner Road, Niagara Falls, ON L2E6S5 Canada

[d]Solvay Metal Extraction Products, 2085 East Technology Circle, Suite 102, Tempe, AZ 85284,USA

Abstract

A combination of mass spectrometry, DFT calculations and $^{31}P\{^1H\}$ NMR spectroscopy has been used to define the mode of action of the commercial cobalt extractant, bis(2,4,4-trimethylpentyl)phosphinic acid (CYANEX®272, $\mathbf{L^1}H$) in Co recovery. The nature of the Co(II)-complexes formed in the water-immiscible phase is determined largely by the propensity of phosphinates to form strong interligand H-bonds in the outer coordination sphere and also to form stable μ_2-Co-O-P-O-Co bridges. At low Co loading levels, the predominant species is the 4:1 complex, $[Co(\mathbf{L^1}.\mathbf{L^1}H)_2]$, in which coordinated neutral phosphinic acid ligands form strong H-bonds to adjacent anionic phosphinates. At higher Co loading, oligomers such as $[(\mathbf{L^1}.\mathbf{L^1}H)Co(\mathbf{L^1}_2Co)_n(\mathbf{L^1}.\mathbf{L^1}H)]$ are formed with μ_2-phosphinate bridging, resulting in a substantial increase in the viscosity of the water-immiscible phase. The presence of tris(2,4,4-trimethylpentyl)phosphine oxide ($\mathbf{L^2}$) in the commercial formulation reduces the viscosity because its incorporation into oligomeric complexes such as $[(\mathbf{L^2})Co\{\mathbf{L^1}_3Co\mathbf{L^1}Co\mathbf{L^1}_3Co\}_m\mathbf{L^1}]$ can terminate chains, resulting in a lower average molecular weight. The uptake of Zn by $\mathbf{L^1}H$ shows a very similar dependence of viscosity on loading, and DOSY spectra and mass spectrometry demonstrate that higher molecular weight species are present at high Zn loading.

Introduction

Society is increasingly dependent on metals to fuel technological advances,[1] and consequently improving processes for their recovery from primary and secondary sources is of great socioeconomic importance.[2]

Cobalt has been widely identified as a 'critical material',[3–5] and, as an overwhelming majority of the world's supply arises as a by-product of nickel and copper production,[5] it is important to develop efficient separation processes for its recovery. Hydrophobic derivatives of phosphorus acids, including the commercially available reagents DEHPA® (the di-2-ethylhexyl ester of phosphoric acid), PC-88A (the 2-ethylhexyl ester of 2-ethylhexylphosphonic acid) and CYANEX®272 (bis(2,4,4-trimethylpentyl)phosphinic acid), are known to show selectivity for Co over Ni in the recovery of these metals by solvent extraction; previous studies have determined cobalt/nickel separation factors of 2.2 and 5 for DEHPA®, 21 and 71 for PC-88A, and values as high as 380, 830 and 2700 for CYANEX®272.[6,7,8]

It is recognized that these reagents form very stable dimers (**II** in Figure 1) in the non-polar hydrocarbon diluents used commercially, and that interligand hydrogen bonding is usually retained when metal cations are bound, leading to the formation of pseudo-chelated structures.[9] This results in the stoichiometry of extraction involving twice the number of phosphorus acid molecules that would be required to generate a charge-neutral, hydrocarbon-soluble, complex (Equation 1) if they were all present as their conjugate anions.
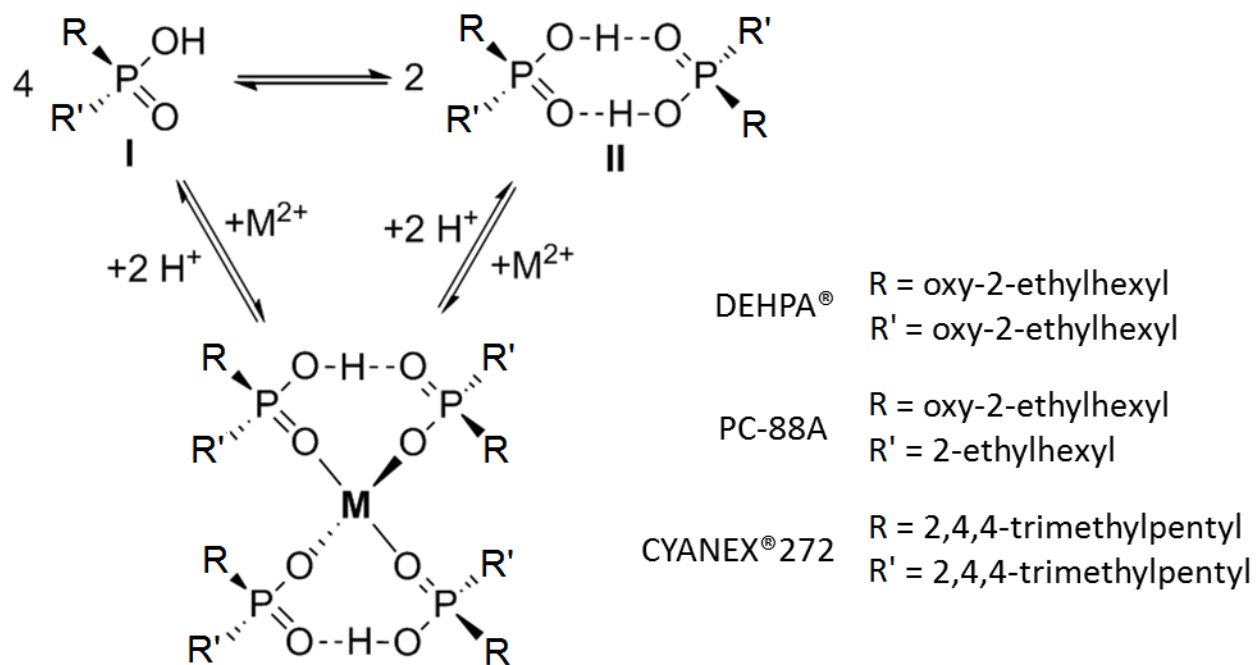

Figure 1. Monomeric (**I**) and dimeric forms (**II**) of phosphorus acid proligands, LH, showing the retention of interligand hydrogen bonding on formation of a charge-neutral tetrahedral complex, $[M(L.LH)_2]$, with M^{2+}.

The pseudo-chelate rings formed by the $[L.LH]^-$ units provide a good fit for tetrahedral 1st transition-metal series dications, which accounts for the selectivity for Co(II) over Ni(II) shown by CYANEX®272.[6,7,8] Similarly, the high selectivity for Zn(II) shown by DEHPA®, applied widely in commercial Zn-recovery,[10] is attributed to the formation of pseudo-chelates of the form $[ZnL_2.LH]$.[11]

$$n[(LH)_2]_{org} + M^{n+} \rightleftharpoons [M(L.LH)_n]_{org} + nH^+ \qquad \text{[Equation 1]}$$
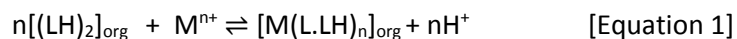
As the application of CYANEX®272 in the separation of cobalt from nickel in sulfate media is of great commercial interest, it has been the subject of a number of literature reports.[12–14] As would be expected for this pH-swing process (Equation 1), higher levels of metal loading into an organic phase are achieved when CYANEX®272 is used to extract metals as the pH of the aqueous phase is increased, but studies have also shown that a significant increase in the viscosity of the water-immiscible phase occurs at high Co loading. As a result, care must be taken to choose appropriate reagent concentrations in order to control viscosity and avoid disrupted flow and slow phase disengagement.

The origins of the increase in viscosity are poorly understood in the context of the supramolecular and coordination chemistry exhibited by CYANEX®272. While solid-state structures of metal complexes of phosphinates are well-defined, and their propensity to form polynuclear species with bridging phosphinate ligands widely reported, the relevance of this phenomenon to solution structures is less well-studied. In the solid state, ten different binding motifs in both mono- and polynuclear complexes have been identified in which an individual phosphinate group can bind up to five metal atoms.[15] Most commonly, phosphinate complexes contain M-O-PR$_2$-O-M units (**a** in Figure 2) in oligomeric and polymeric structures. The implication that similarly high molecular weight complexes are formed in solution is particularly relevant to solvent extraction when metal-loading results in increased viscosity of the organic phase. Formation of 4-membered chelate rings (**b** in Figure 2) is very rare, being recorded only 3 times in solid state structures.
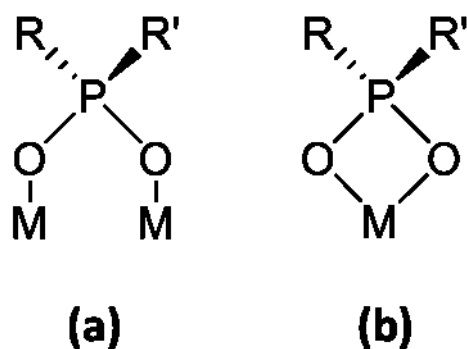

Figure 2. (**a**) The most common binding motif identified in alkyl- or arylphosphinate complexes in the solid state has 260 occurrences compared with just 3 occurrences of the 4-membered chelate structure (**b**) in a total of 552 structures retrieved when the survey of the CCDC was conducted.[15]

While the formation of aggregates at high Co(II) loading levels has been proposed,[16] relatively little experimental evidence of aggregate formation, or of the structures of such aggregates, has been reported. Generally, studies of the solvent extraction of Co(II) from sulfate media using CYANEX®272 have proposed only mononuclear extracted species consisting of Co(II) and hydrogen-bonded dimers of phosphinic acid (Figure 1).[12,13]

Herein, the speciation of the cobalt-compounds formed by CYANEX®272 is considered in the context of the propensity of phosphinate ligands to show unusual supramolecular chemistry based on H-bonding and to form oligomeric complexes rather than simple 4-membered chelate rings (see above). The work involves the application of a wide variety of experimental characterization techniques, including the combination of electrospray ionisation mass spectrometry (ESI-MS) and matrix-assisted laser desorption ionisation time-of-flight (MALDI-TOF) mass spectrometry, along with proton-decoupled ^{31}P NMR spectroscopy of both paramagnetic and diamagnetic complexes and diffusion-ordered NMR spectroscopy (DOSY NMR). These are complemented by computational analysis, with DFT geometry optimization calculations identifying the most stable gas phase Co-containing species and determining the thermodynamic driving forces for their interconversion.

Experimental

Solvents and reagents were used as received from Solvay, Sigma-Aldrich, Fisher Scientific UK, Alfa Aesar, Acros Organics or VWR International. Deionised water was obtained from a Milli-Q purification system.

Reagent definitions: The structures of the main component of CYANEX®272, the phosphinic acid **L¹H,** the phosphine oxide impurity **L²**, and their methyl analogues **L³H** and **L⁴** used in computational studies, are shown in Figure 3.

L¹H	R = R' =	**L²**	R = R' =
L³H	R = R' = Me	**L⁴**	R = R' = Me
L⁵H	R = Ph , R' = H		
L⁶H	R = R' = Ph		

Figure 3. The structures of **L¹H,** the main component of the extractant CYANEX®272 and its phosphine oxide impurity, **L²**. **L³H** and **L⁴** were used as models in computational studies and **L⁵H** and **L⁶H** are present in the solid state structures of [py₃Co(μ₂-**L⁵**)₃CoCl] and [Co(μ₂**L⁶**)₂] discussed below.[17,18]

General Extraction Procedures: All metal stock solutions contained 20 g L^{-1} metal (as CoSO₄•7H₂O, ZnSO₄•7H₂O or anhydrous Fe₂(SO₄)₃ for Co(II), Zn(II) and Fe(III) respectively) in deionised water. Except where otherwise stated, the water-immiscible (organic) phases consisted of 10% (by volume) CYANEX®272 (an extractant consisting of 85% bis(2,4,4-trimethylpentyl)phosphinic acid, along with small quantities of tris(2,4,4-trimethylpentyl)phosphine oxide and other impurities) in the commercial dearomatised kerosene diluent ISOPAR M. In experiments where the concentration of phosphine oxide impurity was varied, this was achieved by substituting varying proportions of CYANEX®272 with CYANEX®272Y (a purer formulation of CYANEX®272 with negligible phosphine oxide content).

4

All volumes were measured with 1 mL and 5 mL Rainin edp3 automatic pipettes. Extraction mixtures consisted of 8 mL organic phase, 4 mL metal stock solution and 4 mL of a mixture of deionised water and either 1 M H_2SO_4 or 1 M NaOH stock solutions, the proportions of which were varied in order to vary the pH of the extraction mixture (monitored using an Ionode IJ44 pH electrode). To perform extractions, mixtures were prepared in vials, sealed, and then subjected to vigorous magnetic stirring at a rate of approximately 900 rotations per minute overnight at room temperature, conditions under which equilibrium is known to be achieved.[8] After separation, both the organic and aqueous phases were centrifuged for 15 minutes to remove entrained material. In some cases, where stated, the organic phase was pre-loaded with low concentrations of Fe(III) by performing an extraction by the procedure described above using Fe(III) stock solution in the aqueous phase, before using the resulting pre-loaded organic phase in a second extraction (of Co(II)) by the same procedure.

Loading levels were determined by measurement of the metal concentrations of aqueous phases (for Co and Zn) and organic phases (for Fe and S), using inductively coupled plasma optical emission spectroscopy (ICP-OES), with a Perkin Elmer Optima 5300DC spectrometer. Aqueous phase samples were diluted 1:400 in 2% nitric acid and taken up by a peristaltic pump at a rate of 1.5 mL min^{-1} into a Gem Tip cross flow nebuliser and a Scotts spray chamber, while organic phase samples were diluted 1:400 in 1-methoxy-2-propanol and taken up by a peristaltic pump at a rate of 2.0 mL min^{-1} into a Gem Tip cross flow nebuliser and a Glass Cyclonic spray chamber. Argon plasma conditions were: 1500 W RF forward power, argon gas flows of 20, 1.4 and 0.45 L min^{-1} for plasma, auxiliary and nebuliser flow, respectively. ICP-OES calibration standards for cobalt, zinc, iron and sulfur were obtained from VWR International or Sigma-Aldrich.

Metal loading levels are reported as percentages, relative to the theoretical maximum quantity of metal which could be extracted by the amount of phosphinic acid present in the organic phase, assuming a 2:1 stoichiometry of phosphinate to metal in the extracted metal complex (see ESI Section S1 for detail).

Viscosity: Viscosities were recorded on a HAAKE MARS rotational viscometer using a constant shear rate of 70 s^{-1} over a period of 60 seconds at 293 K, a gap size of 0.5 mm and a sample volume of 1.45 mL.

NMR spectroscopy: $^{31}P\{^{1}H\}$ NMR and DOSY spectra were recorded on a Bruker PRO500 spectrometer as d^6-benzene solutions. All measurements were performed at 300 K, at a frequency of 202.40 MHz for ^{31}P and 500.12 MHz for ^{1}H. Spectra were analysed using the MestReNova software.[19]

For Co extraction, peak integrals were calculated as a means of quantifying the relative proportions of species present in the organic phase. Assuming **L²** to be insignificantly involved in the extracted cobalt species below high loading levels, the ratio of the integrals of the peaks corresponding to unassociated **L¹H** and **L²** was used to monitor the change in proportion of **L¹** associated to cobalt as Co loading increases. By comparison with the known absolute concentrations of unassociated **L¹H** in the organic phase at 0% loading and of Co in the organic phase at 100% loading, the proportion of unassociated **L¹H** versus Co uptake in the organic phase was calculated, and the stoichiometries of extracted species inferred (see ESI Section S2 for detail).

Mass spectrometry: Electrospray ionisation mass spectra (ESI-MS) were recorded on a Bruker 12 T SolariX mass spectrometer, with samples diluted into a 3:1 mixture of methanol and chloroform. MALDI-TOF mass spectra were recorded on a Bruker UltraflexExtreme mass spectrometer, with solutions of sample (1 mg mL^{-1} in chloroform) mixed with solutions of dithranol (20 mg mL^{-1} in chloroform) in a 1:10 ratio before spotting on the sample plate. Spectra were analysed using the Bruker Compass DataAnalysis software, with peaks assigned manually.

Computational Methods

All geometry optimisation calculations were performed using the Gaussian 09 software package.[20] The M06 functional was used in all calculations,[21] along with the LANL2DZ basis set and its associated pseudopotential for Co and the 6-31+G* basis set for all other atoms.[22] Structures were considered optimised when the standard convergence criteria (maximum force of 4.5×10^{-4} Hartrees/Bohr on any atom, maximum RMS force of 3.0×10^{-4} over all atoms, maximum atomic displacement of 1.8×10^{-3} Bohr for any atom, and maximum RMS atomic displacement of 1.2×10^{-3} Bohr over all atoms) were reached.

Results and Discussion

Cobalt loading and organic-phase viscosity

As much of the experimental work in this study involves comparison of the behaviour of organic-phase CYANEX®272 solutions at different levels of Co loading in a solvent extraction experiment, it was essential to devise protocols such that loading levels were reproducible. The pH-dependence of Co loading was established through a series of test extractions at varying pH (Figure 4) and these data dictated the amounts of acid or base required to obtain samples of particular Co loading levels for subsequent measurements.
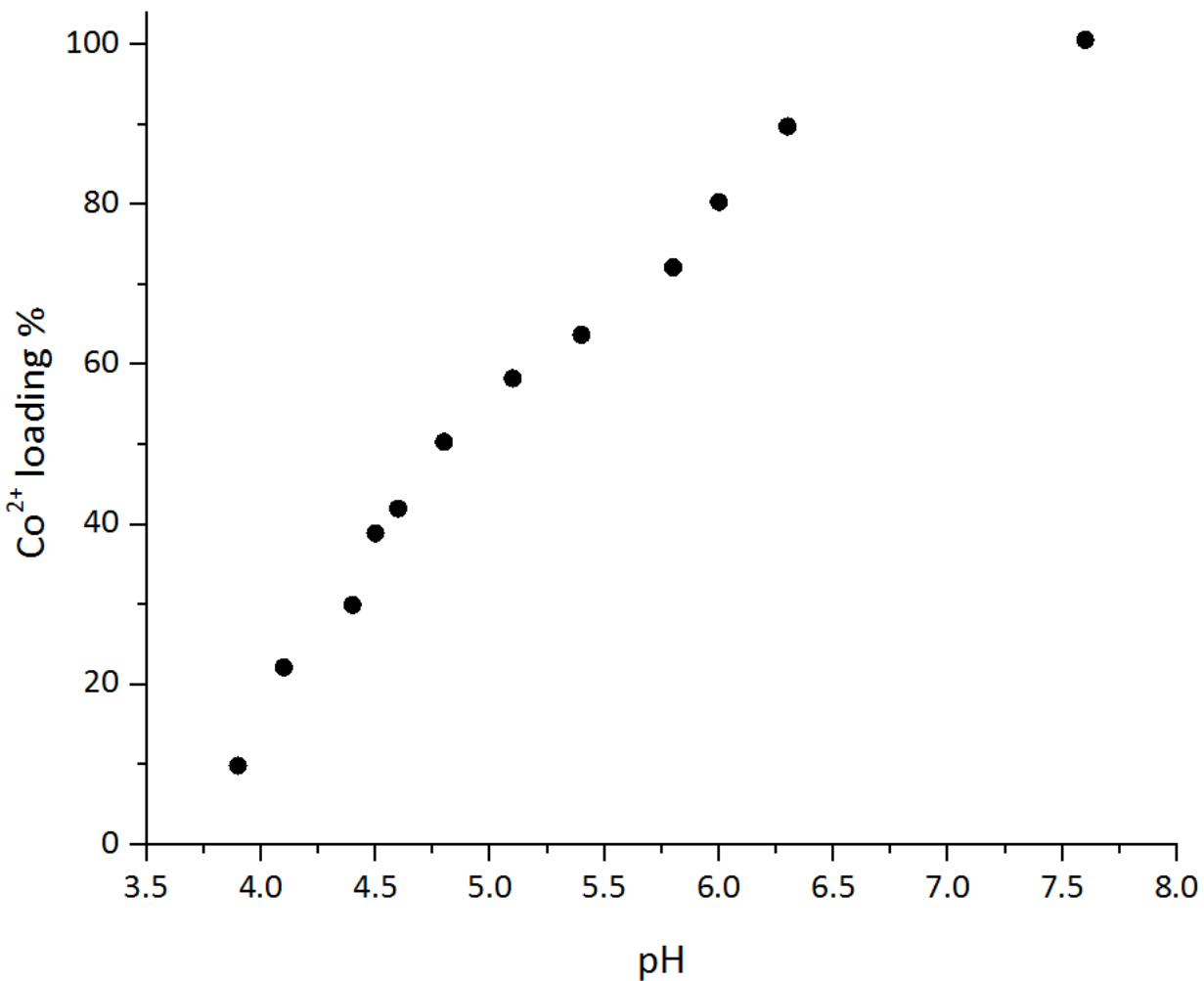
Figure 4. The pH dependence of loading of Co(II) from an aqueous phase into an organic phase of CYANEX®272 (0.27 M) in ISOPAR M.

In common with other reports,[16] viscosity levels of the organic phase were found to rise sharply when Co-loading exceeded 80%. Very similar behavior was observed with the loading of Zn^{2+} [see Figure 5(a)].
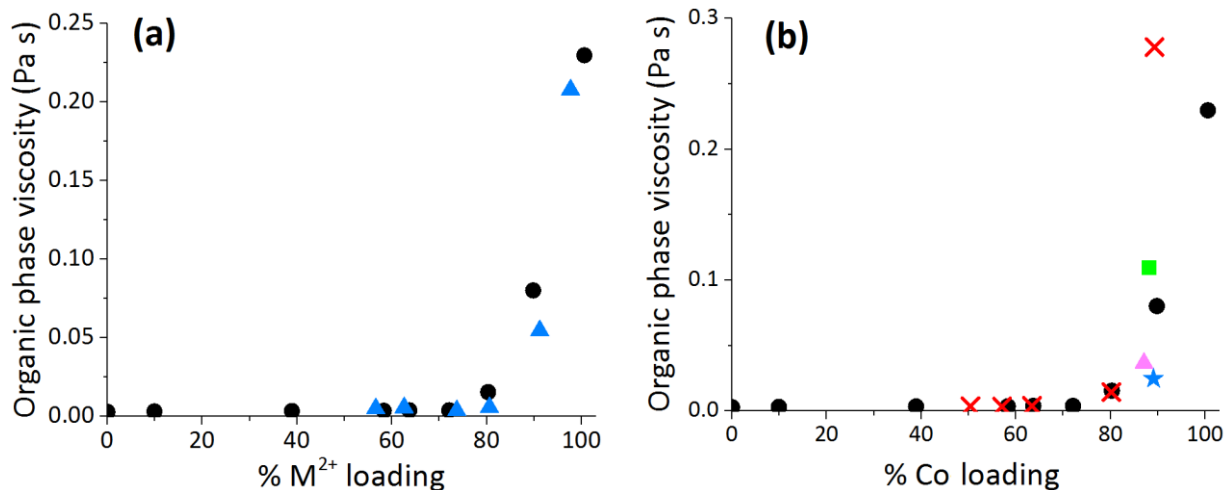
Figure 5. The variation of viscosity of **(a)** CYANEX®272 in ISOPAR M loaded with Co (black circles) and Zn (blue triangles) and **(b)** ISOPAR M containing mixtures of CYANEX®272 and CYANEX®272Y in proportions of 100% CYANEX®272:0% CYANEX®272Y (black dots), 75%:25% (green squares), 50%:50% (pink triangles), 25%:75% (blue stars) and 0%:100% (red crosses), at varying Co loading levels.

The role of the impurities in CYANEX®272 (ca. 10%) was explored by repeating extractions using CYANEX®272Y, which contains negligible quantities of the phosphine oxide L^2 (Figure 3). The CYANEX®272Y solution in ISOPAR M was diluted to ensure that it contained the same molar concentration (0.27 M) of the phosphinic acid, L^1H, as corresponding solutions of CYANEX®272. The extractant formulation containing no phosphine oxide, L^2, produced very similar viscosity levels at low Co loading levels to those using formulation containing L^2, but once the critical loading level of 80%, had been reached, the subsequent rise in viscosity was considerably greater [Figure 5(b)]. This effect was investigated further by mixing CYANEX®272Y in different proportions with CYANEX®272 (whilst maintaining a consistent concentration of the phosphinic acid extractant L^1H). The extractant formulations containing greater proportions of CYANEX®272Y (and therefore lower quantities of L^2) exhibited higher levels of viscosity [Figure 5(b)].

In order to determine the solution structures of the species responsible for high viscosity at high Co loading, various methods were applied to define the stoichiometry of the Co complexes formed in the water-immiscible phase.

NMR analysis of extraction

As the phosphinic acid L^1H and the phosphine oxide impurity L^2 each contain only a single phosphorus environment, $^{31}P\{^1H\}$ NMR spectroscopy offers the means to analyse the relative concentrations of species present in the organic phase. The $^{31}P\{^1H\}$ NMR spectrum for CYANEX®272 was recorded [Figure 6(**a**)] and showed an intense singlet at 58 ppm corresponding to the phosphinic acid, L^1H, accompanied by a much smaller singlet at 46 ppm due to the phosphine oxide impurity L^2. The resonance corresponding to L^2 was not detected in the $^{31}P\{^1H\}$ NMR spectrum of CYANEX®272Y (see ESI, Figure S3).

The $^{31}P\{^1H\}$ NMR spectra of organic phases containing CYANEX®272 after loading with varying quantities of Co(II) showed dramatic changes (Figure 6). At 42% Co loading, the signal due to **L^{1}H** was noticeably broadened and at 58% loading was hard to detect (spectra **b** and **c**). At that point, it can be assumed that all phosphinic acid, **L^{1}H**, was bound to the paramagnetic Co^{2+} ion. The signal due to **L^2** remained sharp at 42% Co loading, suggesting that none was bound to Co(II), although there was a shift to lower frequency associated with the change in bulk susceptibility of the solvent. No other $^{31}P\{^1H\}$ resonances were observed in the range -1000 to 1000 ppm at any the Co loading levels examined. At 58% Co loading, the signal for **L^2** was broadened, and at 90% Co loading it was no longer detected. This is believed to be a consequence of the build-up of paramagnetic material in the system as Co loading reaches high levels, rather than incorporation of **L^2** in Co(II) complexes, as the signal due to **L^2** did not disappear in this manner at high loading in similar experiments involving diamagnetic Zn(II) (see Figure 8).
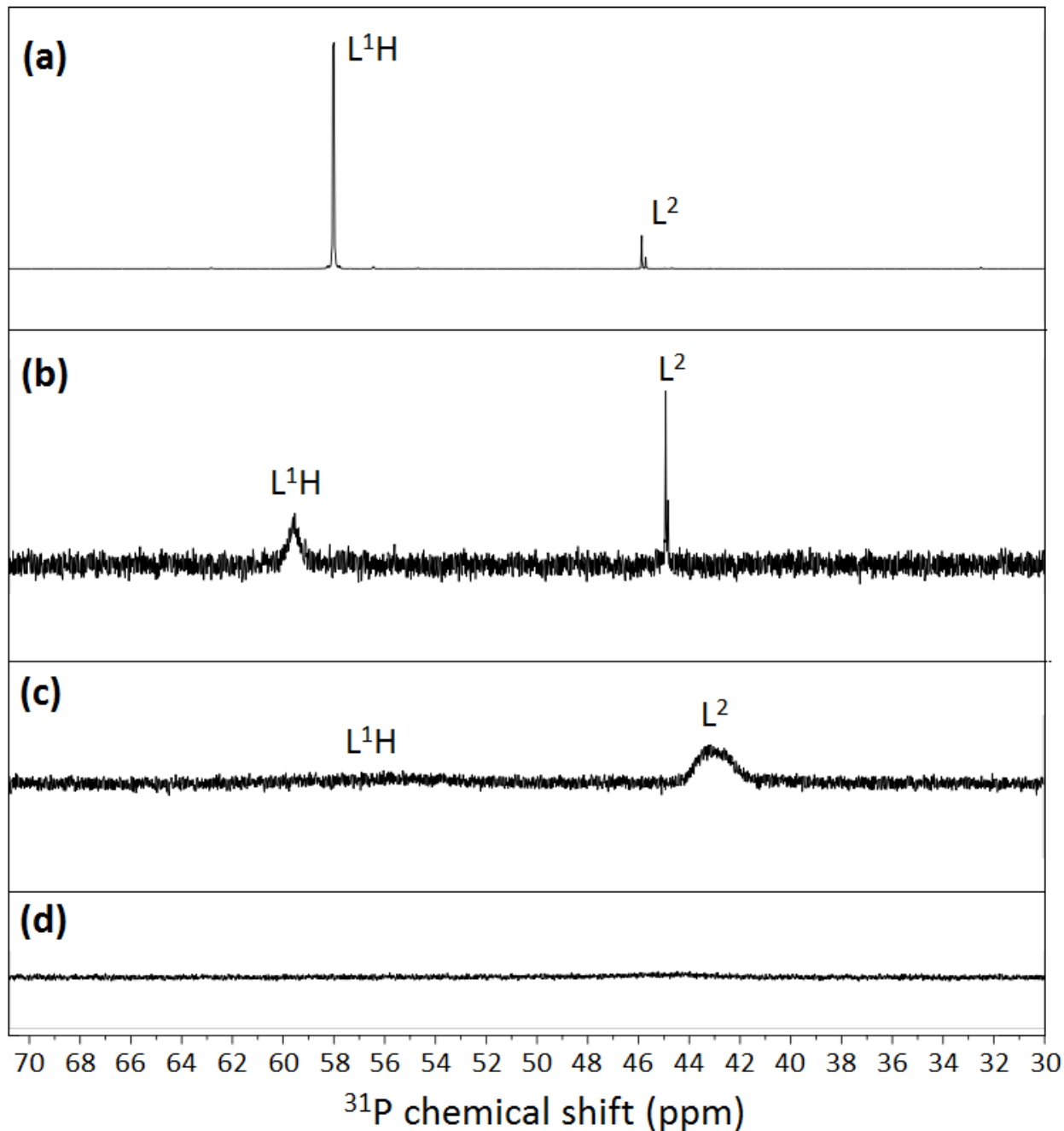
Figure 6. $^{31}P\{^1H\}$ NMR spectra obtained from ISOPAR M solutions of CYANEX®272 with **(a)** zero Co loading, **(b)** 42% Co loading, **(c)** 58% Co loading, and **(d)** 90% Co loading.

If the assumptions are made that the phosphine oxide impurity, **L²**, does not contribute significantly to the formation of extracted cobalt species at loading levels, below that at which viscosity begins to rise, and that peak suppression due to residual paramagnetism affects both signals proportionately, then the ratio of the area of the **L¹H** signal to that of the **L²** signal can be used to evaluate the proportion of the uncomplexed phosphinic acid at a given (low) Co loading level. The proportion of free phosphinic acid, **L¹H**, remaining in the organic phase does not vary linearly with Co uptake, with consumption of **L¹H** being

greater at low (< 50%) Co loading (see Figure 7). The mean gradient of the graph in the range of 0-20% Co loading corresponds to the consumption of 3.92 moles of phosphinic acid for every mole of Co(II) transferred into the organic phase, and suggests that, at low Co concentration, the 4:1 ligand:metal complex [Co($L^1.L^1H$)$_2$] is formed (see Figure 1). Similar calculations for the Co loading in the range 20-60% suggest that on average 2.42 moles of phosphinic acid are consumed per mole of Co(II) extracted, consistent with the presence of a mixture of the mononuclear complex [Co($L^1.L^1H$)$_2$] and polynuclear complexes with formulae such as [(L^1H)Co(L^1)$_3$Co(L^1)].

The integral of the resonance due to L^1H (and thus the L^1H:L^2 integral ratio) reaches zero at a Co loading level of around 70%, which is close to the critical Co loading level above which organic phase viscosity begins to rise rapidly. This supports the notion that the onset of the increase in viscosity occurs when Co loading reaches such a level that there is no free L^1H in the system to allow further formation of mononuclear and small polynuclear species.

The incorporation of the phosphine oxide L^2 into oligomeric complexes could increase the total Co uptake as all the phosphinic acid is present as its conjugate anion [L^1]$^-$ and the resulting complexes have a 1:2 Co:L^1 molar ratio. A corollary is that identical Co loadings will be associated with lower (average) molecular weights when L^2 is part of the complex formed. This is consistent with the lower viscosity being observed when CYANEX®272, which contains 10% phosphine oxide, L^2, is used as the extractant (see Figure 5).
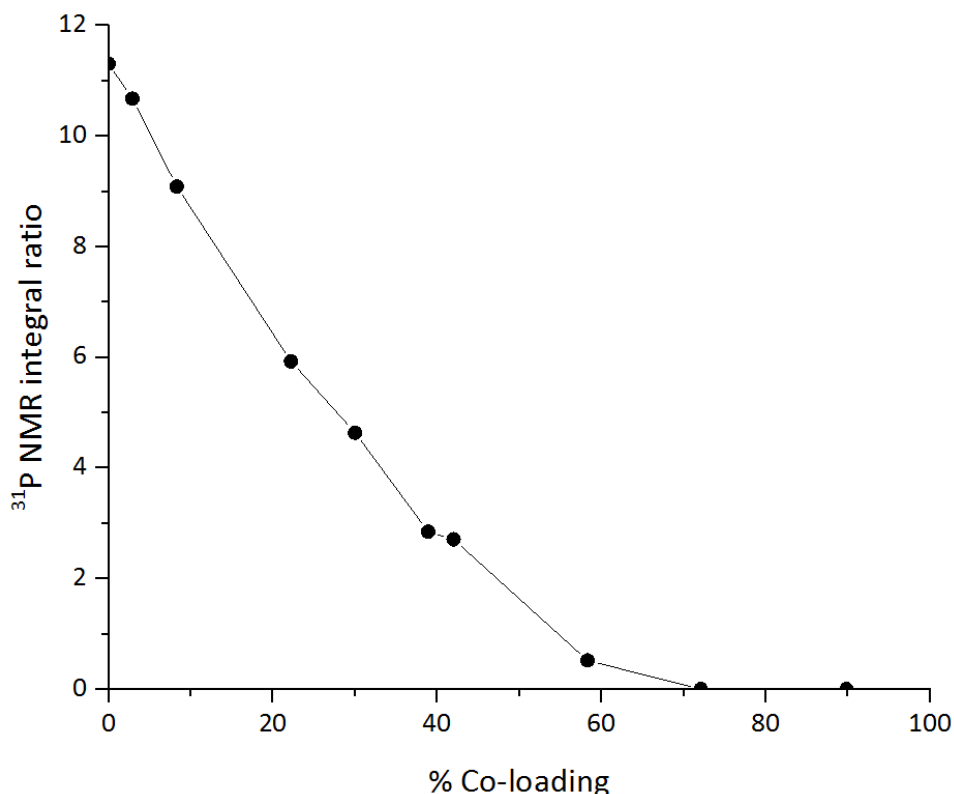

Figure 7. The ratio of the integrals of peaks L^1H and L^2 in $^{31}P\{^1H\}$ NMR spectra of ISOPAR M solutions of CYANEX®272 with different levels of Co loading.

Diffusion-ordered NMR spectroscopy (DOSY) could be used to investigate whether high molecular weight compounds are formed under conditions that result in high Co loading. However, as complexes of Co(II)

are paramagnetic, studies of the uptake of Zn(II) by CYANEX®272 were undertaken, as this metal showed a similar loading profile and viscosity dependence on loading levels to those for Co(II) (see Figure 5).

The diffusion coefficients (which vary inversely with the hydrodynamic radius of the corresponding species) were determined as a function of the chemical shifts of $^{31}P\{^{1}H\}$ signals for solutions of CYANEX®272 loaded with varying levels of Zn(II) (Figure 8). Resonances labelled **A** and **B** correspond to **L^1**H and **L^2** in metal-free CYANEX®272. At 18% Zn loading, an additional resonance (**C**) of lower intensity and a higher hydrodynamic radius was observed which can be ascribed to a Zn-containing complex. At 69% Zn loading, resonance **A** was absent (no uncomplexed phosphinic acid, **L^1**H, remained) and two new resonances (**D** and **E**) appeared. These had different chemical shifts but identical diffusion coefficients, suggesting that they were due to two different phosphorus environments within a single oligomer. At 90% Zn loading, well above the critical level at which viscosity began to rise substantially, two further broad resonances (**F** and **G**) can be seen. These arise from compounds of significantly higher hydrodynamic radii, which is consistent with much larger oligomers being formed at high Zn loading. Generally, the intensity of resonance **G** is greater at lower values of diffusion coefficient than that of resonance **F**, indicating that the phosphorus environment responsible for resonance **G** occurs disproportionately in polymers of relatively low molecular weight. It is possible that resonance **G** corresponds to units of the phosphine oxide **L^2** which have become incorporated into the polymer structure, terminating the growth of the polymer and thus creating lower molecular-weight species. This provides an explanation for the observation that the inclusion of **L^2** in the organic phase moderates the increase in organic phase viscosity seen at high metal-loading levels (see Figure 5(b)).
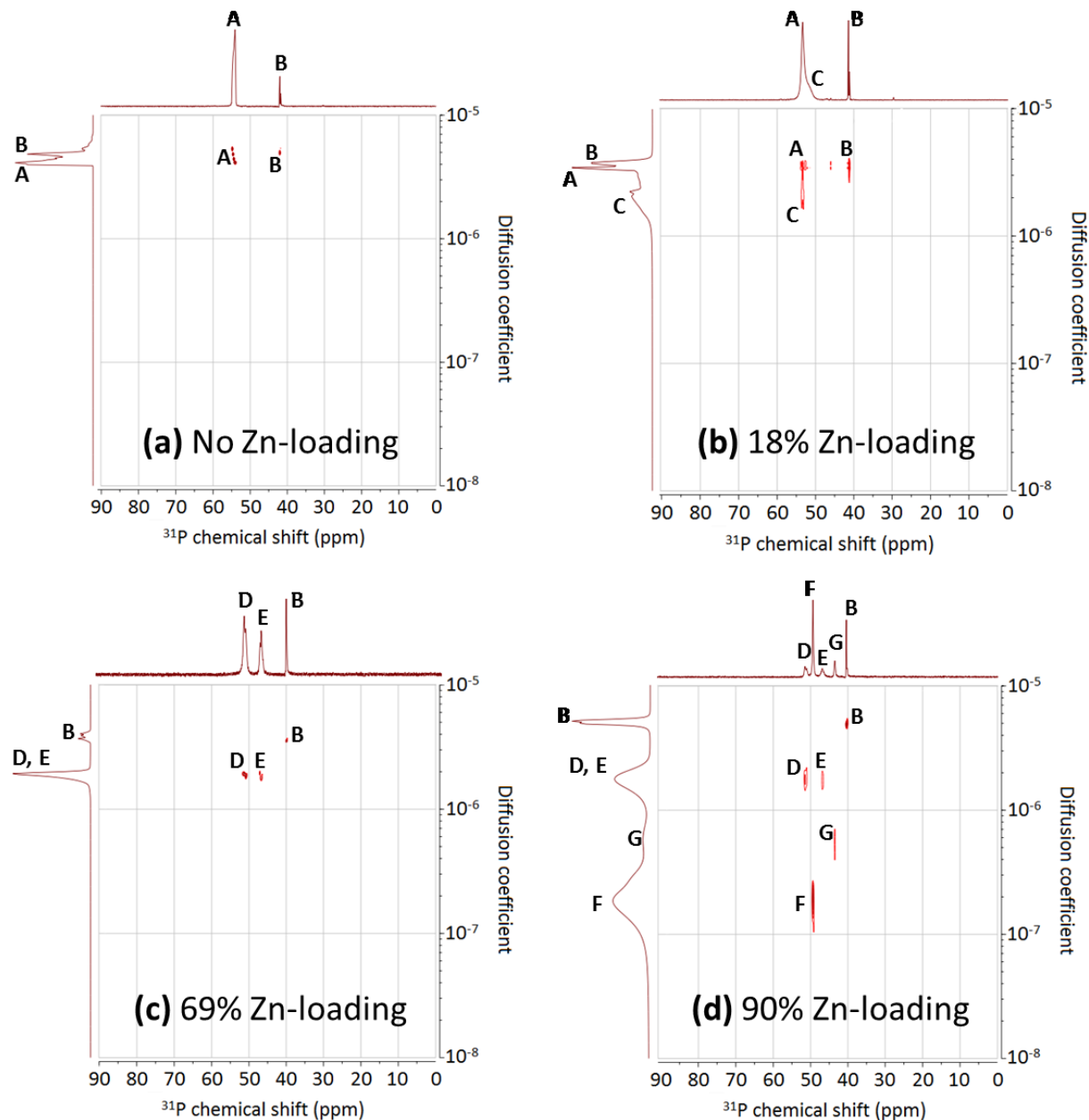
Figure 8. DOSY spectra; plots of diffusion coefficient against $^{31}P\{^1H\}$ NMR chemical shift for solutions of CYANEX®272 with zero, 18%, 69% and 90% Zn loading (**a** to **d** respectively).

Mass Spectrometry

The ESI-MS of an organic phase solution with 42% Co loading was recorded (Figure 9) and no major ions with m/z > 1800 were observed. The ion at m/z 1218.9 was assigned to a protonated form of the mononuclear complex [Co(**L¹.L¹**H)$_2$] which was assumed to be the dominant species at low Co loading. [12,13]
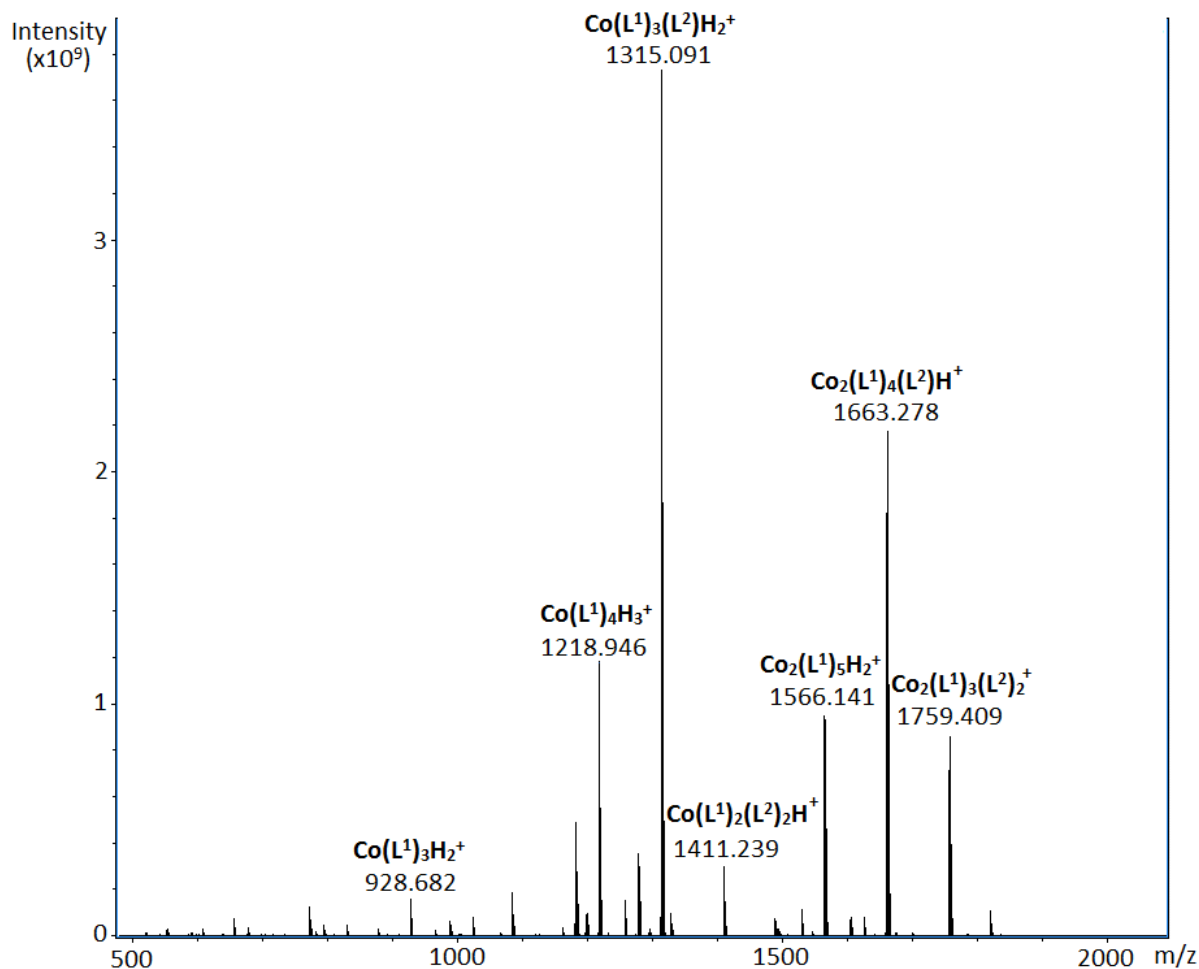
Figure 9. Positive-ion ESI-MS obtained from an organic phase with 42% Co loading of CYANEX 272.

The ion of m/z 1566.1 contains two Co atoms and five L^1 units, and is most plausibly formulated as $[(L^1H)Co(L^1)_3Co(L^1H)]^+$ with three bridging phosphinates and two capping phosphinic acids. The linking of two Co(II) atoms with three bridging phosphinate ligands was observed in the solid state structure of $[py_3Co(\mu_2\text{-}L^5)_3CoCl]$.[17] A dinuclear complex of this nature, with both bridging and terminal L^1 units, is likely to be responsible for the resonances **D** and **E** in DOSY NMR spectra at medium and high loading (see Figure 8). This is supported by the observation of exactly equivalent peaks in ESI-MS spectra of Zn-loaded organic phases (see ESI Section S6).

The ions of m/z 1315.1, 1411.2, 1663.3 and 1759.4 can only be assigned with chemically reasonable formulae if one or two L^1 units in $[Co(L^1.L^1H)_2]^+$ or $[(L^1H)Co(L^1)_3Co(L^1H)]^+$ are replaced by the phosphine oxide L^2, resulting in ions of empirical formulae $[Co(L^1)_3(L^2)H_2]^+$, $[Co(L^1)_2(L^2)_2H]^+$, $[Co_2(L^1)_4(L^2)H]^+$ and $[Co_2(L^1)_3(L^2)_2]^+$ (Figure 9). A curious feature of this mass spectrum is that ions containing the phosphine oxide L^2 have disproportionally high intensities compared with the concentration of L^2 in CYANEX®272 as used in the extraction. The possibility that L^2 is generated by disproportionation of L^1H in the ESI-MS apparatus can be discounted because much lower intensities of L^2-containing peaks are found in spectra using the 'pure' reagent CYANEX®272Y and there is no evidence in the mass spectrum for the formation

14

of 2,4,4-trimethylpentylphosphonic acid. A more credible alternative is that **L²**-containing cationic complexes are more stable or more readily generated in the electrospray ionization process.

Further evidence for the formation of oligomeric/polymeric complexes at high Co loading is found in the MALDI-TOF mass spectrum of 100% Co-loaded CYANEX®272 in a chloroform/dithranol matrix (Figure 10). Ions of m/z 985.9, 1623.3 and 2260.6 can be assigned to fragments of the oligomers $[(\mathbf{L^1}.\mathbf{L^1H})Co\{(\mathbf{L^1})_2Co\}_n(\mathbf{L^1}.\mathbf{L^1H})]$ with a repeat unit of $[Co(\mathbf{L^1})_2]$ (formulae $[Co_2(\mathbf{L^1})_3]^+$, $[Co_3(\mathbf{L^1})_5]^+$, and $[Co_4(\mathbf{L^1})_7]^+$ respectively) formed at high Co loading. The proposition that complexes of generic formula $[Co_n(\mathbf{L^1})_{n+1}]^+$ are formed by fragmentation of a polymer during the ionization process is supported by the observation that the intensity of the higher m/z $[Co_n(\mathbf{L^1})_{n+1}]^+$ peaks increases relative to that of the lower m/z peaks when the laser power is reduced.
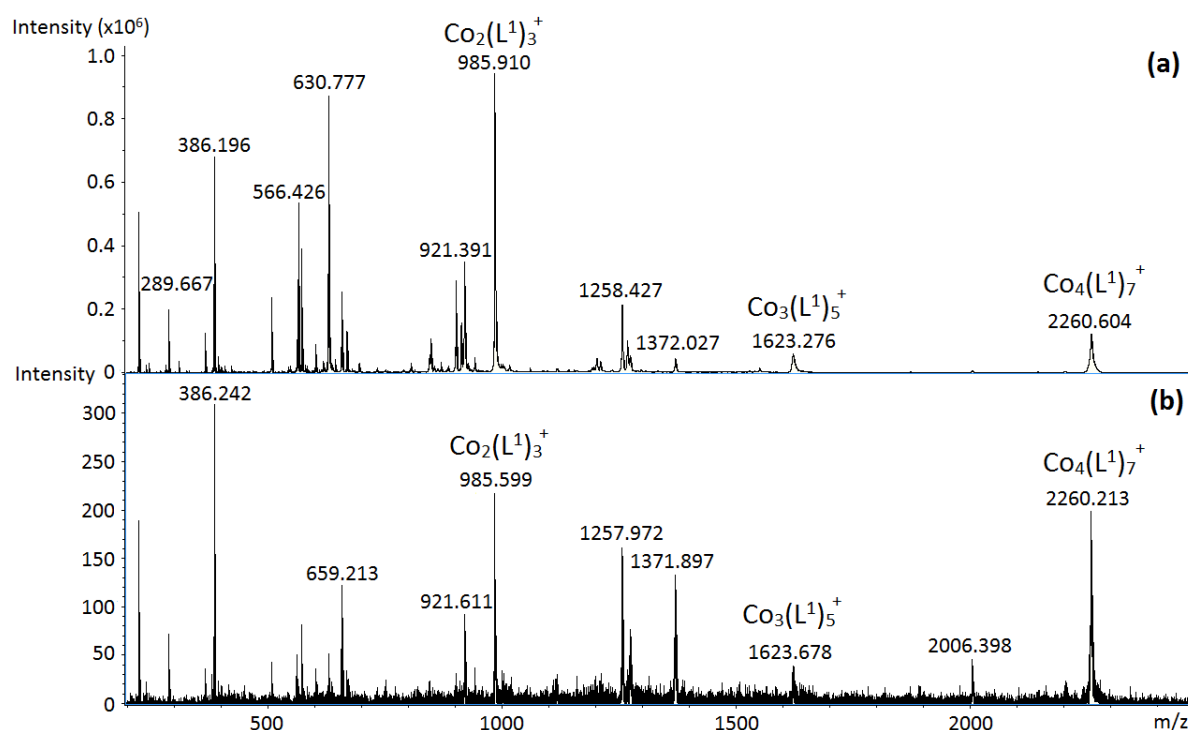

Figure 10. MALDI-TOF mass spectra obtained from a highly viscous organic phase containing CYANEX®272 with Co^{2+} loaded to a level of 100%, using laser power settings of **(a)** 70% and **(b)** 1%.

Prominent peaks could be assigned to the fragments $[Zn_2(\mathbf{L^1})_3]^+$ and $[Zn_4(\mathbf{L^1})_7]^+$ in a spectrum of a viscous Zn-loaded sample (see ESI Section S7), indicating that a similar oligomerisation occurs at high Zn loading, and supporting the assignment of the low-diffusivity species observed in DOSY analysis (Figure 8**(d)**) to oligomeric species.

As the formation of oligomeric, phosphinate-bridged, species is of considerable significance to the efficiency of Co-transfer in commercial operations, it is appropriate to consider what factors could influence the effective concentration of **L¹**H under various operating conditions. As mentioned above, it appears that the phosphine oxide **L²** can replace **L¹**H as end groups in oligomers at very high Co loadings and thus increase the effective concentration of extractant. The uptake of anions such as SO_4^{2-}, HSO_4^- or OH^- from the aqueous phase and incorporation into complexes in the organic phase could also achieve

this. There is some evidence that sulfate is transferred in the extraction of copper, based on the Cu-loading dependence on sulfate concentration,[23] but in this work no evidence for the presence of SO_4^{2-} or HSO_4^- was found by mass spectrometry or by ICP-OES analysis of organic phases.

Computational analysis:

DFT calculations were undertaken in order to assess the stability of the various complexes proposed above, and to rationalise their formation. For the purposes of these calculations, the phosphinic acid **L^{1}H** and phosphine oxide **L^2** were replaced by their methyl-substituted analogues, **L^{3}H** and **L^4,** respectively (see Figure 3) in order to reduce computational expense associated with differentiating between very large numbers of conformers of the 2,4,4-trimethylpentyl groups in CYANEX®272. The thermodynamic stability of [Co(**L^3.L^{3}H**)$_2$], used as a model for the mononuclear cobalt-containing species formed at low Co loading of CYANEX®272, was compared to that of the mononuclear complex containing two bidentate phosphinate ligands, [Co(**L^3**)$_2$], see Figure 11), by evaluating the internal energy charge associated with the reaction expressed in Equation 2:

$$[\text{Co}(\mathbf{L^3})_2] + (\mathbf{L^3H})_2 \rightleftharpoons [\text{Co}(\mathbf{L^3}.\mathbf{L^3H})_2] \qquad [\text{Equation 2}]$$
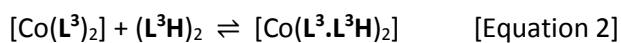
The internal energy of [Co(**L^3.L^{3}H**)$_2$] was calculated to be 112.6 kJ mol^{-1} lower than the sum of the internal energies of the compounds on the left hand side of Equation 2, indicating a strong thermodynamic impetus for the reaction to proceed in the forward direction (see ESI Section S4 for calculated energy values). Phosphinic acid dimers (LH)$_2$ are generally accepted to be the lowest-energy forms of free phosphinic acids (in hydrocarbon solution),[15] which suggests that the overwhelming difference in internal energy between the two sides of Equation 2 results from the instability of [Co(**L^3**)$_2$]. An explanation for this is that the phosphinate ligands are insufficiently flexible to allow for O-Co-O angles close to the ideal tetrahedral angle (109.5°) when in their bidentate co-ordination mode; the bite angles defined by the oxygen atoms in [Co(**L^3**)$_2$] were found to be only 74.6°. In contrast, the O-Co-O angles in the optimised geometry of [Co(**L^3.L^{3}H**)$_2$] deviate from the ideal tetrahedral angle by only 4.8° on average, accounting for its much greater stability. These results are consistent with the rarity of solid-state structures containing the 4-membered chelate ring (see Figure 2).[15]

It is recognized that the calculation of the energy of the gas phase reaction shown in Equation 2 takes no account of differences in solvation energies, which will likely influence the reaction equilibrium in solution. However, these differences are likely to be small in a non-polar solvent such as ISOPAR M because the polar and H-bond donor groups in the complexes and the proligand dimer will be effectively shielded by the 2,4,4-trimethylpentyl groups present in CYANEX®272.
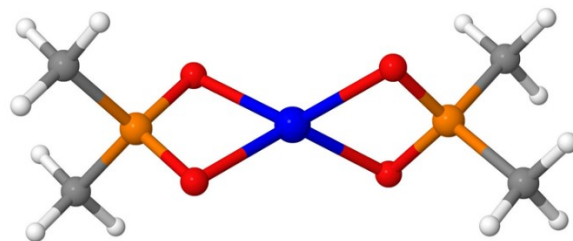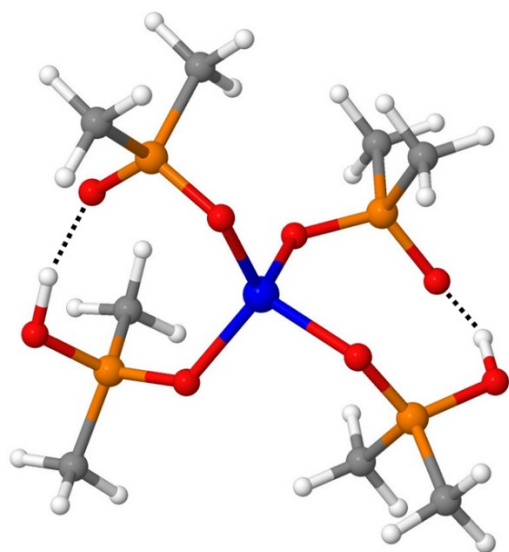
$Co(\mathbf{L^3}.\mathbf{L^3}H)_2$ $Co(\mathbf{L^3})_2$

Figure 11. Energy-minimised structures of [Co($\mathbf{L^3}.\mathbf{L^3}$H)$_2$] (left) and the hypothetical complex [Co($\mathbf{L^3}$)$_2$] (right). Hydrogen bonds are indicated by dotted lines. Co: blue, P: orange, O: red, C: grey, H: white

Optimised geometries of the methyl analogues of the cationic complexes with empirical formulae [Co($\mathbf{L^1}$)$_3$($\mathbf{L^2}$)H$_2$]$^+$, [Co$_2$($\mathbf{L^1}$)$_4$($\mathbf{L^2}$)H]$^+$ and [Co$_2$($\mathbf{L^1}$)$_3$($\mathbf{L^2}$)$_2$]$^+$ (Figure 12), proposed as the structures of the ions observed by ESI-MS (Figure 9) with m/z 1566.1 1663.3 and 1759.4 respectively, were obtained. All optimized structures were found to contain O-Co-O bond angles in the range of 98.3-116.8°, close to the ideal tetrahedral geometry favoured by Co(II) ions (see ESI Section S5).
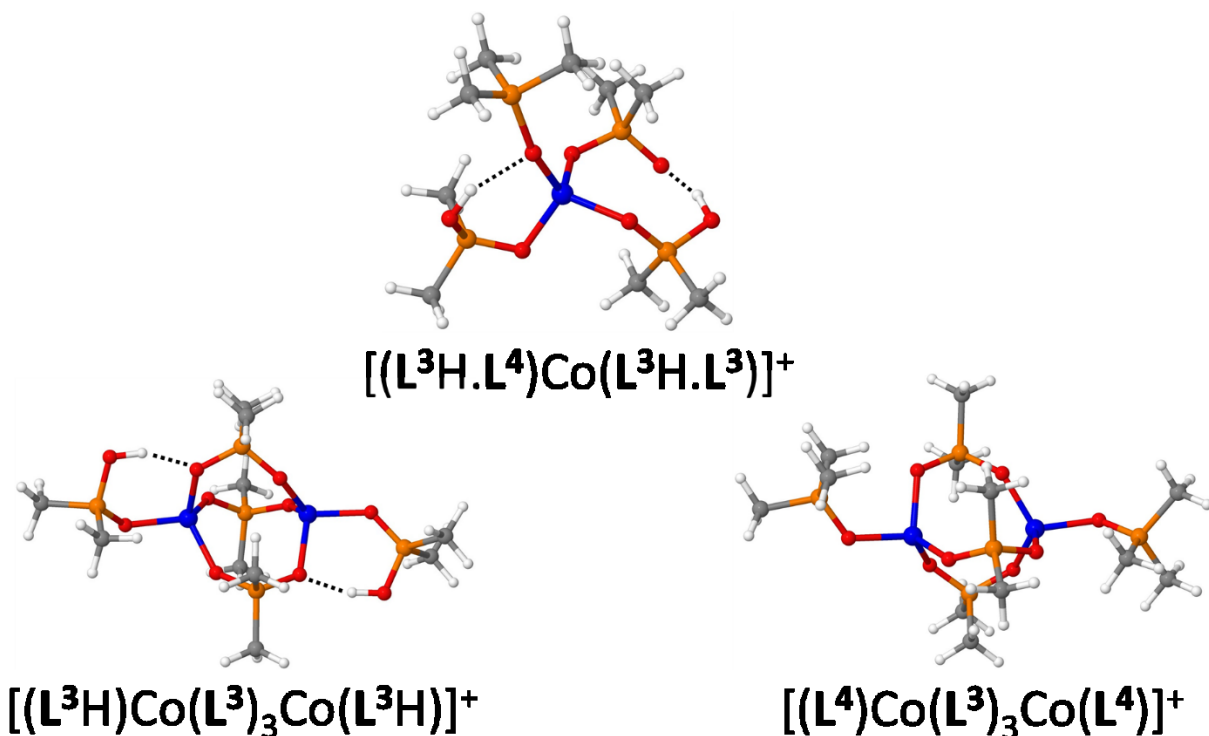
Figure 12. Energy-minimised structures of [(**L³**H. **L⁴**)Co(**L³.L³**H)]⁺, [(**L³**H)Co(**L³**)₃Co(**L³**H)]⁺ and [(**L⁴**)Co(**L³**)₃Co(**L⁴**)]⁺, the methyl-substituted models for ions with empirical formulae [Co(**L¹**)₃(**L²**)H₂]⁺, [Co₂(**L¹**)₅H₂]⁺ and [Co₂(**L¹**)₃(**L²**)₂]⁺ (m/z 1315.1, 1566.1 and 1759.4) in the ESI-MS spectrum in Figure 9. Hydrogen bonds are indicated by dotted lines.

Repeat units containing the symmetrical μ_2-bridging mode (see Figure 2(a)) were found to provide bond angles even closer to those favoured by tetrahedral metal ions. In the solid state structure of [Co₂(μ_2-**L⁶**)₂], the bridging phenylphosphinate ligands define O-Co-O angles in the range 104.3-116.4°.[18] Similar geometries are found in the repeat units of the geometry-optimised (gas phase) structures of the dinuclear [(**L³.L³**H)Co(**L³**)₂Co(**L³.L³**H)] and the trinuclear [(**L³.L³**H)Co{(**L³**)₂Co}₂(**L³.L³**H)] (Figure 13). Angles subtended by the oxygen atoms in the pseudochelating units (**L³.L³**H)⁻ fall in the range of 108.2-115.5° and those by the bridging phosphinate ligands in the range 107.9-112.2°. The possibility of adopting such favourable co-ordination geometries is likely to be a thermodynamic driving force towards the formation of complexes of this form.
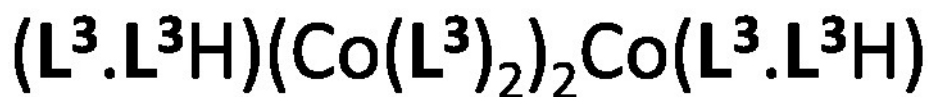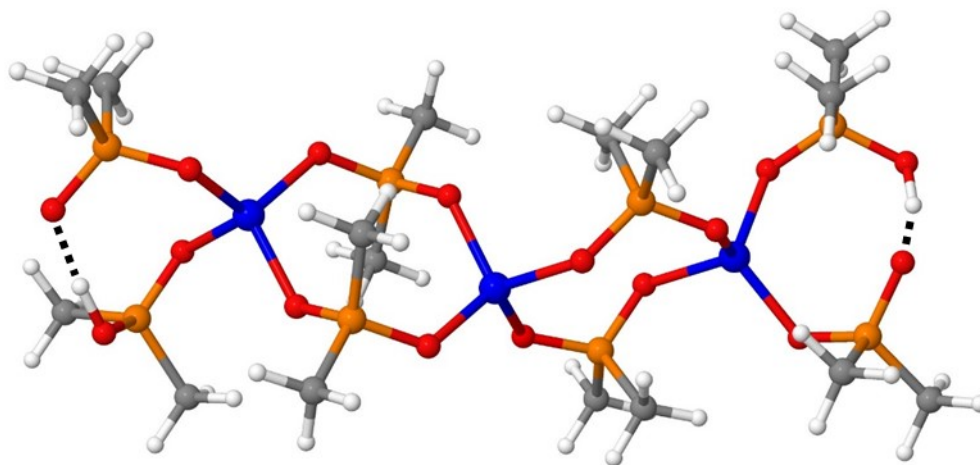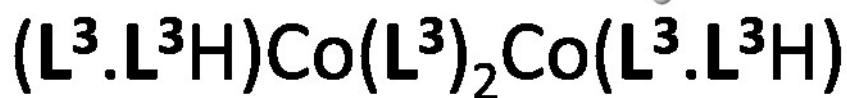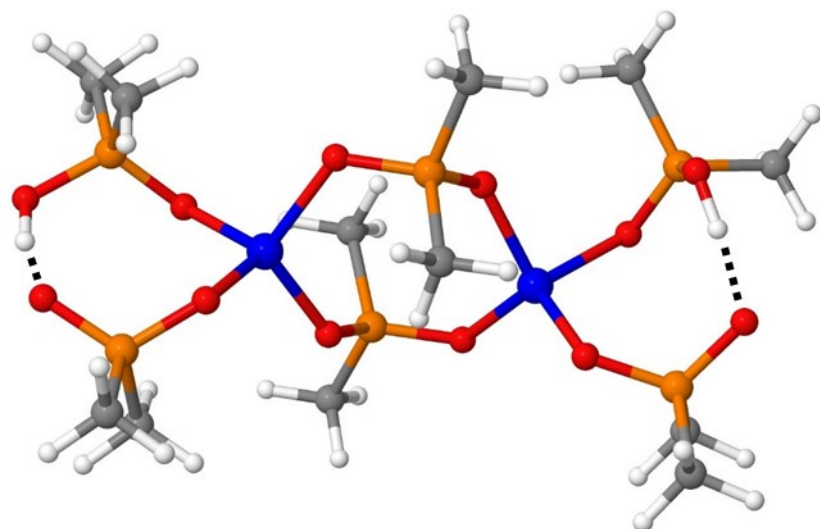
$$(\mathbf{L^3}.\mathbf{L^3}H)Co(\mathbf{L^3})_2Co(\mathbf{L^3}.\mathbf{L^3}H)$$

$$(\mathbf{L^3}.\mathbf{L^3}H)(Co(\mathbf{L^3})_2)_2Co(\mathbf{L^3}.\mathbf{L^3}H)$$

Figure 13. Energy-minimised structures of the di- and trinuclear complexes [(**L³.L³H**)Co(**L³**)₂Co(**L³.L³H**)] and [(**L³.L³H**)Co{(**L³**)₂Co}₂(**L³.L³H**)]. Hydrogen bonds are indicated by dotted lines.

Fe(III) pre-loading:

As CYANEX®272 readily forms stable complexes with Fe(III) cations,[24] the presence of Fe(III) in feed solutions should reduce the concentration of **L¹H** available to Co and therefore increase the viscosity of the organic phase at lower Co loading compared to an Fe(III)-free system. This was shown to be the case

by carrying out solvent extraction of Co into organic phases that were pre-loaded with low concentrations of Fe(III) (Figure 14). In this case, the presence of Fe(III) caused the viscosity of the organic phase to increase at lower Co loading (<80%), which is likely due to the loss of **L^{1}H** in the formation of organic-soluble Fe(III) phosphinate complexes. The requirement for a 3:1 phosphinate:Fe(III) stoichiometry to generate a charge neutral species in the organic phase compounds compounds this problem.
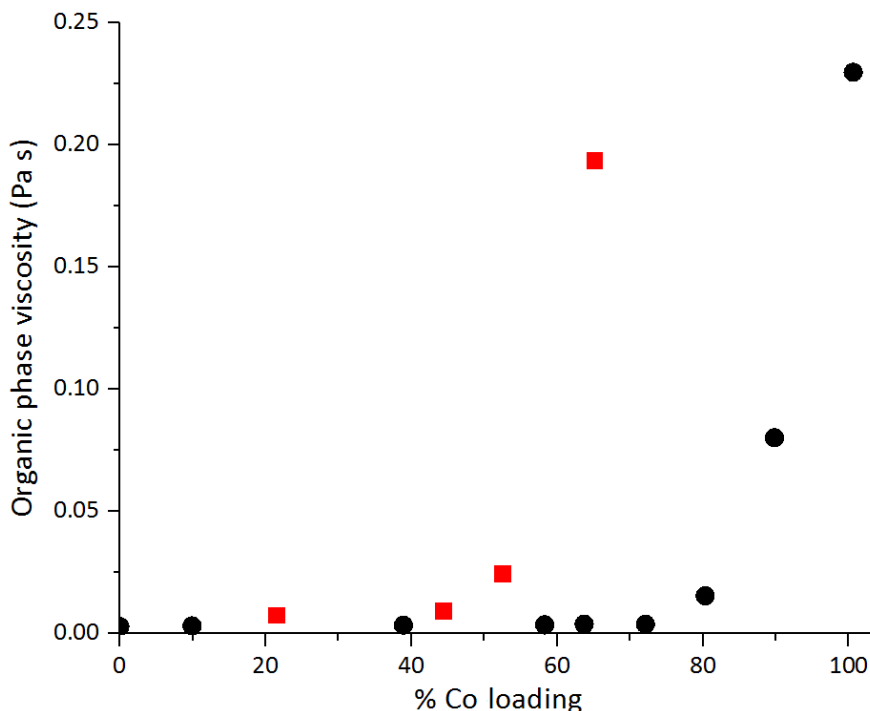

Figure 14. A comparison of the variation in the viscosity with Co loading by a CYANEX®272 solution in ISOPAR M when preloaded to a level of 27% (of the theoretical limit assuming 2:1 **L^1**:M stoichiometry) with Fe^{3+} (red squares) and in the absence of Fe(III) (black circles).

The dependence of ^{31}P{^{1}H} NMR shifts on Co loading (as in Figure 6) was measured for samples in which the organic phase had been 'pre-loaded' with low concentrations of Fe(III) (Figure 15). As expected, the presence of Fe(III) decreased the proportion of "free" phosphinic acid, **L^{1}H**, relative to phosphine oxide **L^2** in solution. ICP-OES analysis of the aqueous phase following extraction of cobalt into an organic phase pre-loaded with iron confirmed that no iron was displaced into the aqueous phase upon Co loading. As such, the presence of Fe(III) in the Co-containing leach solution will decrease the Co extraction capacity of CYANEX®272 due to preferential coordination of Fe cations by the phosphinic acid.
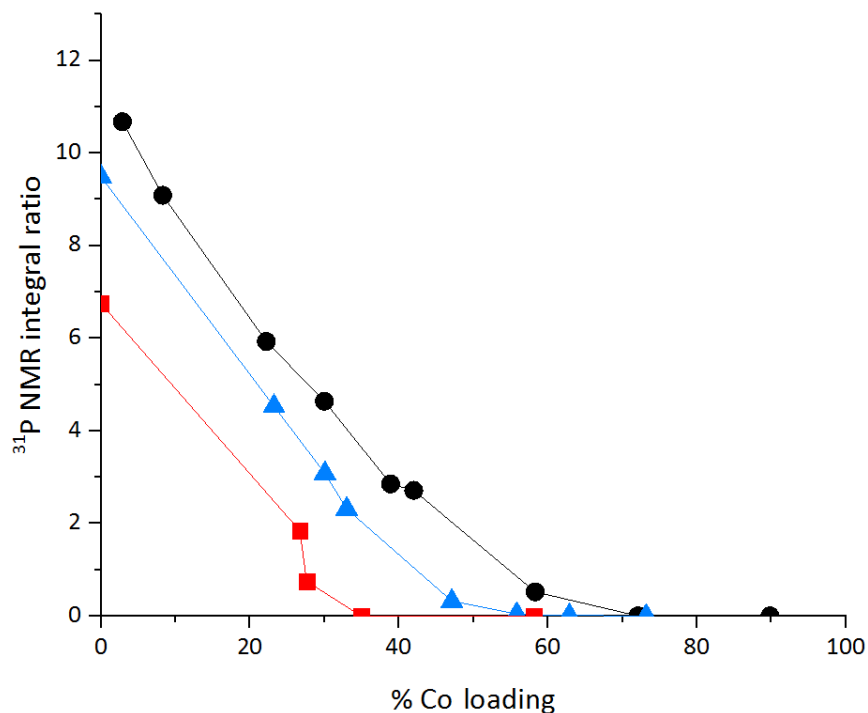
Figure 15. The variation in the ratio of the integrals of peaks **L^1**H and **L^2** in ^{31}P{^{1}H} NMR spectra with increasing Co loading for CYANEX®272 solutions in ISOPAR M which were pre-loaded with Fe(III) to levels of 0% (black circles), 6% (blue triangles) and 27% (red squares).

Conclusions

The unusual features of Co-recovery by phosphinic acids such as CYANEX®272 in solvent extraction processes (abrupt viscosity increase at high loading and L:M change from 4:1 to 2:1) can be accounted for in terms of two key aspects of the coordination and supramolecular chemistry of phosphinic acids: (i) the propensity to form outer-sphere hydrogen-bonding interactions between ligands in Co(II) complexes, leading to "pseudo-chelate" rings which favour tetrahedral coordination geometry (Figure 1) and (ii) the propensity to form M-O-P-O-M bridges between metal centres (Figure 2a). As Co-loading increases, the decreasing availability of neutral phosphinic acid favours the replacement of the pseudochelating hydrogen-bonded motif found in mononuclear complexes with the bridging motif, which leads to the formation of polynuclear Co(II) complexes and causes a major increase in the viscosity of the organic phase.

The broadening of the signal for coordinated phosphinic acid **L^1**H due to the paramagnetism of Co(II) permits the use of ^{31}P{^{1}H} NMR spectroscopy to infer the extent of complex formation between the phosphinic acid and Co(II) by comparing the integrals of the signals arising from **L^1**H and the phosphine oxide modifier **L^2**, which is not incorporated into Co(II) complexes until very high Co loading is achieved.

The assignment of empirical formulae to ions in the ESI and MALDI-ToF mass spectra of Co-loaded solutions of CYANEX®272, combined with the computation of energy-minimised structures, provides very plausible structures for both mononuclear and polynuclear complexes formed as loading levels are increased. All of these are consistent with the phosphinic acid and, at high Co loading, the phosphine oxide components being able to present an unstrained tetrahedral O$_4$-donor set for the cobalt cation. ^{31}P{^{1}H}

NMR spectra of Zn(II)-loaded solutions provide evidence for the formation of increasingly higher molecular weight species, consistent with increasing viscosity at high Zn loading which follows a similar profile to that of Co loading.

In general there is a striking similarity between the extraction behaviour of Co(II) and Zn(II) when using CYANEX®272, in particular the dependence of viscosity on metal loading. This is consistent with the coordination chemistries of these metals being similar, especially when forming complexes with hard, anionic ligands.[25,26] Co(II) has been used for some time as a structural probe for the active sites of zinc-containing enzymes when replacing this "spectroscopically silent" metal ion,[27] and this technique continues to find favour.[28] In most cases the Co(II)-substituted enzymes retain their catalytic properties. As might be expected from the Irving Williams order,[25,29] the apparent stability constants for Zn(II) binding to proteins are consistently slightly higher than those for Co(II) binding.[27] The similarities of the coordination chemistry of cobalt and zinc do not extend to oxidizing conditions or to systems containing high field ligands which promote the formation of Co(III). This ion, which is kinetically inert,[30,31] usually forms octahedral complexes which in solvent extraction, for example using the commercial phenolic oxime reagents,[32] are very difficult to strip. Phosphinate ligands do not favour the formation of Co(III) and all the cobalt complexes found in the Cambridge X-ray structural database contain Co(II). Several such complexes are structurally identical to their zinc analogues, e.g. ALELIM and ALEKAD,[33] and XAXJUC and XAXKAJ.[34]

Whilst all the techniques described above provide results consistent with the proposed changes in speciation which lead to increased viscosity at high metal loadings they do not provide definitive structures for the complexes formed. The plausibility of the proposed structures formed in hydrocarbon solutions is supported by DFT calculations which demonstrate that these gas phase structures have very similar features to the most commonly observed structures in the solid state.[15]

Conflicts of interest

There are no conflicts to declare.

Acknowledgements

References

1   G. Rodich and G. R. Matos, *The Global Flows of Metals and Minerals*, 2008, https://pubs.usgs.gov/of/2008/1355/pdf/ofr2008-1355.pdf (accessed July 2017)

2   *Resources That Don't Cost the Earth*, 2011, http://www.rsc.org/globalassets/04-campaigning-

outreach/tackling-the-worlds-challenges/resources-that-dont-cost-the-earth.pdf (accessed July 2017)

3   *Resource security action plan: making the most of valuable materials*, 2012, https://www.gov.uk/government/uploads/system/uploads/attachment_data/file/69511/pb13719-resource-security-action-plan.pdf (accessed July 2017)

4   *Tackling the Challenges in Commodity Markets and on Raw Materials*, 2011, http://eur-lex.europa.eu/legal-content/EN/TXT/PDF/?uri=CELEX:52011DC0025&from=EN (accessed July 2017)

5   *Critical Materials Strategy*, 2010, https://energy.gov/sites/prod/files/piprod/documents/cms_dec_17_full_web.pdf (accessed July 2017)

6   P. R. Danesi, L. Reichley-Yinger, G. Mason, L. Kaplan, E. P. Horwltz and H. Diamond, *Solvent Extr. Ion Exch.*, 1985, **3**, 435–452.

7   T. Zhu, in *International Solvent Extraction Conference*, 2002, pp. 203–207.

8   *CYANEX®272 Extractant*, Cytec Industries Inc., 2008.

9   M. J. Nicol, C. A. Fleming and J. S. Preston, *Comprehensive Coordination Chemistry, vol. 6*, 1987.

10   P. M. Cole, *Miner. Process. Extr. Metall. Rev.*, 2003, **24**, 91–137.

11   C. I. Sainz-Diaz, H. Klocker, R. Marr and H.-J. Bart, *Hydrometallurgy*, 1996, **42**, 1–11.

12   J. S. Preston, *Hydrometallurgy*, 1982, **9**, 115–133.

13   B. K. Tait, *Hydrometallurgy*, 1993, **32**, 365–372.

14   D. Maljkovic, Z. Lenhard and M. Balen, *EMC '91: Non-Ferrous Metallurgy - Present and Future*, 1991.

15   I. Carson, M. R. Healy, E. D. Doidge, J. B. Love, C. A. Morrison and P. A. Tasker, *Coord. Chem. Rev.*, 2017, **335**, 150–171.

16   F. Xun and J. A. Golding, *Solvent Extr. Ion Exch.*, 1987, **5**, 205–226.

17   J. S. Maass, M. Zeller, T. M. Breault, B. M. Bartlett, H. Sakiyama and R. L. Luck, *Inorg. Chem.*, 2012, **51**, 4903–4905.

18   R. Winpenny, E. Brechin, S. Parsons and D. Messenger, *CSD Commun.,* 2014.

19   MestReNova version 11.0.1-17801, 2016, MestreLab Research

20   Gaussian 09, Revision A.02, M. J. Frisch, G. W. Trucks, H. B. Schlegel, G. E. Scuseria, M. A. Robb, J. R. Cheeseman, G. Scalmani, V. Barone, G. A. Petersson, H. Nakatsuji, X. Li, M. Caricato, A. V. Marenich, J. Bloino, B. G. Janesko, R. Gomperts, B. Mennucci, H. P. Hratchian, J. V. Ortiz, A. F. Izmaylov, J. L. Sonnenberg, D. Williams-Young, F. Ding, F. Lipparini, F. Egidi, J. Goings, B. Peng, A. Petrone, T. Henderson, D. Ranasinghe, V. G. Zakrzewski, J. Gao, N. Rega, G. Zheng, W. Liang, M. Hada, M. Ehara, K. Toyota, R. Fukuda, J. Hasegawa, M. Ishida, T. Nakajima, Y. Honda, O. Kitao, H. Nakai, T. Vreven, K. Throssell, J. Montgomery, J. A., J. E. Peralta, F. Ogliaro, M. J. Bearpark, J. J. Heyd, E. N. Brothers, K. N. Kudin, V. N. Staroverov, T. A. Keith, R. Kobayashi, J. Normand, K.

Raghavachari, A. P. Rendell, J. C. Burant, S. S. Iyengar, J. Tomasi, M. Cossi, J. M. Millam, M. Klene, C. Adamo, R. Cammi, J. W. Ochterski, R. L. Martin, K. Morokuma, O. Farkas, J. B. Foresman and D. J. Fox, Gaussian, Inc., Wallingford CT, 2009 2016.

21   Y. Zhao and D. G. Truhlar, *Theor. Chem. Account.*, 2008, **120**, 215–241.

22   P. J. Hay, W. R. Wadt, P. J. Hay and W. R. Wadt, *J. Chem. Phys.*, 1985, **82**, 299–310.

23   R. K. Biswas and H. P. Singha, *Indian J. Chem. Technol.*, 2007, **14**, 269–275.

24   R. K. Biswas and H. P. Singha, *Hydrometallurgy*, 2006, **82**, 63–74.

25   J. J. R. Frausto da Silva and R. J. P. Williams, *The Biological Chemistry of the Elements, Second Edition*, Oxford University Press, 2001.

26   K. F. Purcell and J. C. Kotz, *Inorganic Chemistry*, Saunders, 1977.

27   W. Maret and B. L. Vallee, *Methods Enzymol.*, 1993, **226**, 52–71.

28   E. Shumilina, O. Dobrovolska, R. Del Conte, H. W. Holen and A. Dikiy, *J. Biol. Inorg. Chem.*, 2014, **19**, 85–95.

29   H. Irving and R. J. P. Williams, *J. Chem. Soc.*, 1953, **0**, 3192–3210.

30   K. F. Purcell and J. C. Kotz, *Inorganic Chemistry*, Saunders, 1977.

31   J. E. Huheey, *Inorganic Chemistry: Principles of Structure and Reactivity*, Harper & Row, 3rd edn., 1983.

32   J. Szymanowski, *Hydroxyoximes and Copper Hydrometallurgy*, CRC Press, 1993.

33   V. Kubíček, P. Vojtíšek, R. J, P. Hermann and I. Lukeš, *Dalt. Trans.*, 2003, 3927–3938.

34   V. Chandrasekhar, R. Boomishankar, P. Sasikumar, L. Nagarajan and A. W. Cordes, *Zeitschrift Für Anorg. Und Allg. Chemie*, 2005, **631**, 2727–2732.

Table of Contents Graphic

$^{31}P\{^1H\}$ NMR spectroscopy, ESI-mass spectrometry and DFT calculations elucidate solution structures of Co(II) phosphinate complexes which account for increased viscosity at high Co-loading in solvent extraction by Cyanex® 272.